

BRIEF COMMUNICATION



WILEY

Arothron: An R package for geometric morphometric methods and virtual anthropology applications

Profico Antonio¹ | Buzi Costantino^{2,3} | Castiglione Silvia⁴ |
Melchionna Marina⁴ | Piras Paolo⁵ | Veneziano Alessio⁶ | Raia Pasquale⁴

¹PalaeoHub, Department of Archaeology, Hull York Medical School University of York, Heslington, United Kingdom

²Dipartimento di Biologia Ambientale, Sapienza Università di Roma, Rome, Italy

³DFG Center for Advanced Studies “Words, Bones, Genes, Tools”, Universität Tübingen, Rümelinstraße, 23, 72070, Tübingen

⁴Dipartimento di Scienze della Terra, dell'Ambiente e delle Risorse, Università di Napoli Federico II, Naples, Italy

⁵Dipartimento di Ingegneria Strutturale e Geotecnica, Sapienza Università di Roma, Via Eudossiana, 18, Rome, 00184, Italy

⁶14 John Maurice Close, London, SE17 1PZ, United Kingdom

Correspondence

Profico Antonio, PalaeoHub, Department of Archaeology, Hull York Medical School University of York, Heslington, United Kingdom.

Email: antonio.profico@york.ac.uk

Abstract

Objectives: The statistical analysis of fossil remains is essential to understand the evolution of the genus *Homo*. Unfortunately, the human fossil record is straight away scarce and plagued with severe loss of information caused by taphonomic processes. The recently developed field of Virtual Anthropology helps to ameliorate this situation by using digital techniques to restore damaged and incomplete fossils.

Materials and methods: We present the package Arothron, an R software suite meant to process and analyze digital models of skeletal elements. Arothron includes tools to digitally extract virtual cavities such as cranial endocasts, to statistically align disarticulated or broken bony elements, and to visualize local variations between surface meshes and landmark configurations.

Results: We describe the main functionalities of Arothron and illustrate their usage through reproducible case studies. We describe a tool for segmentation of skeletal cavities by showing its application on a malleus bone, a Neanderthal tooth, and a modern human cranium, reproducing their shape and calculating their volume. We illustrate how to digitally align a disarticulated model of a modern human cranium, and how to combine piecemeal shape information on individual specimens into one. In addition, we present useful visualization tools by comparing the morphological differences between the right hemisphere of the Neanderthal and the modern human brain.

Conclusions: The Arothron R package is designed to study digital models of fossil specimens. By using Arothron, scientists can handle digital models with ease, investigate the inner morphology of 3D skeletal models, gain a full representation of the original shapes of damaged specimens, and compare shapes across specimens.

KEYWORDS

3D-imaging, Arothron, digital models, endocast, fossils, human evolution, virtual restoration

This is an open access article under the terms of the Creative Commons Attribution License, which permits use, distribution and reproduction in any medium, provided the original work is properly cited.

© 2021 The Authors. *American Journal of Physical Anthropology* published by Wiley Periodicals LLC.

1 | INTRODUCTION

The study of the human fossil record is essential to understand the evolutionary links connecting fossil species, and them to us (Wood & Richmond, 2000). Unfortunately, this scientific enterprise is complicated by the fact that human fossil remains are rare, not easily accessible, and ought to be handled with great care, which hinders the scope of investigation within the anthropological community. Still, the correct understanding of past phenotypic diversity needs the proper mathematical description of the extinct phenotypes, which is problematic given that most human fossils usually come with extensive distortions and breakages (Gunz et al., 2009). The virtual restoration of partial and/or damaged fossil items can provide a more realistic understanding of the patterns of trait evolution (Joy et al., 2016; Webster & Purvis, 2002), gaining improved knowledge over abstract reconstruction of ancestral states based on a manifold of evolutionary models (Castiglione et al., 2020; Schnitzler et al., 2017; Slater et al., 2012). Therefore, virtual restoration can facilitate the study of phenotypic evolution in the human evolutionary tree. In recent years, the development of new technologies and methods and ever-increasing computational power are widening research frontiers on fossil items (Cunningham et al., 2014; Pandolfi et al., 2020), moving evolutionary studies toward a full, better-informed appreciation of past phenotypic diversity. The institution of “Virtual Anthropology” points exactly toward this direction (Weber, 2001). In Virtual Anthropology the fossil specimens are digitally acquired making it possible to investigate anatomical structures in detail, thus allowing unrestrained manipulation while preserving the integrity of fossil specimens, and making them accessible to a wider than ever before audience of scientists.

TABLE 1 Main functions of the Arothron package

Function	Description	Tool
ext.int.mesh	Find visible vertices from a set of points of view	CA-LSE, AST-3D
out.inn.mesh	This function separates a 3D mesh subjected to the ext.int.mesh into two 3D models: the visible mesh and the not visible one	CA-LSE, AST-3D
endomaker	Build endocast from a skull 3D mesh	endomaker
volendo	Calculate the volume of a mesh by using a voxel-based method	endomaker
dta	Applies the digital alignment tool (DTA) on a disarticulated model using a reference sample	DTA
twodviews	Combine the morphological information from multiple landmark configurations defined on the same items	combinland
twodvarshape	Calculate the shape variations from a twodviews object	combinland
localmeshdiff	Plot the differences in area between two meshes	

The R package Arothron presents brand-new tools for geometric morphometric methods specifically designed for applications in Virtual Anthropology. The functions embedded in Arothron (Table 1) permit to align disarticulated fragments belonging to a single specimen (e.g., a damaged skull); to isolate internal cavities such as endocasts, to reproduce and analyze the shapes of 3D objects; to combine morphological information contained in different landmark coordinate sets into one and to compare 3D models and visualize local shape differences (see Supplementary Code—Install Arothron). We supply several data examples (Table 2) and case studies embedded in Arothron.

2 | MATERIALS AND METHODS

2.1 | Tools for extraction of virtual cavities: CA-LSE, AST-3D, and endomaker

CA-LSE and AST-3D are two new tools designed for the isolation of surface shell and the reconstruction of inner cavities (Profico et al., 2018). CA-LSE provides the reconstruction of the external surface of a 3D mesh by simulating the action of a laser scanner. The algorithm automatically defines N points of view around the mesh to

TABLE 2 Main data embedded in the Arothron package

Data set	Description	Example
DM_base_sur	3D mesh of the first part of the <i>Homo sapiens</i> disarticulated model	DTA
DM_face_sur	3D mesh of the second part of the <i>Homo sapiens</i> disarticulated model	DTA
DM_set	Landmark configurations of the two-part of the disarticulated model	DTA
RMs_sets	Array containing the landmark coordinates of the reference sample for Digital Alignment Tool example	DTA
endo_set	POVs defined inside the endocranial cavity	AST-3D
femsets	Array containing the landmark coordinates of 21 human femora	CScoreffect
human_skull	3D mesh of a human skull	CA-LSE, AST-3D, endomaker
krd1_tooth	3D mesh of a deciduous Neanderthal tooth	CA-LSE
malleus_bone	3D mesh of a human malleus bone	CA-LSE
primendoR	Semilandmark configurations of the right hemisphere belonging to primates and fossil hominins species.	localmeshdiff

be scanned. At each iteration, a spherical flipping operator (Katz et al., 2007) is applied and only the vertices visible from the point of view are selected, effectively rendering the external shape of the object.

AST-3D performs the digital reconstruction of anatomical cavities such as endocasts, and the hollow cavity of bones. In this case, the operator needs to define a set of coordinates within the anatomical structure to be scanned. Each coordinate acts as a point of view; the inner mesh facets visible from at least one of the points of view will define the entire scanned anatomical cavity.

endomaker is an automatic tool for digital endocast production. It works by providing a CT-scan derived cranial mesh as the only input (Profico et al., 2020). *endomaker* locates the cranial endocast cavity by calculating the local density of the mesh vertices. The function returns the mesh of the endocast and calculates its volume, by discretizing the volume defined by the endocranial cavity into voxels of adjustable (by the user) size.

In Arothron, we supply three examples of virtual cavities reconstructions (Figure 1): the dental pulp cavity within a deciduous Neanderthal tooth, the network of blood vessels within a human malleus bone, and an endocast of a human skull (see Supplementary Code—Virtual Cavities) (Profico, 2020).

2.2 | Combining morphological information from a 3D disarticulated model or from landmark configurations: The digital alignment tool and *combinland*

When fossils come broken into disarticulated fragments a preliminary realignment of the remains is often necessary. The digital alignment tool (DTA) is a landmark-based method capable to perform a digital alignment of two portions of a 3D mesh by using a reference sample for comparison (Profico, Piras, et al., 2019). DTA quantifies the morphological distance (i.e., Euclidean distance or Procrustes distance) between each fragment of the disarticulated model and the corresponding portions on each item of the reference sample. The corresponding portions on the reference sample are defined by the user specifying the arguments *mod_1* and *mod_2*. The landmark configurations of each item of the reference sample are scaled at the same centroid size of each part of the disarticulated model. The specimen showing the greatest morphological affinity is automatically selected as reference, and it is then

scaled to the dimension of the disarticulated model and a rigid rotation is applied returning a 3D model suitable for morphological analysis. Importantly, the disarticulated pieces need not cover the entire original shape to apply DTA, meaning that the realignment is possible even if the fossil specimen is incomplete. The DTA case study embedded in Arothron (Figure 2) consists of a simulated case study in which a complete human skull has been virtually disarticulated into two portions (see Supplementary Code—DTA) (Profico, 2020).

In Geometric Morphometrics, shapes are defined by sets of anatomical (landmarks) and/or geometric (semi-landmarks) points. In some cases, the shape information is acquired from different anatomical views (e.g., sample of images on different views) or as 2D views (pictures) of 3D objects, or referring to different regions of a single structure (e.g., periosteum and endosteum). A solution to retrieve the shape information for the overall anatomical part under investigation is to combine the morphological data coming from two or more views belonging to the same specimen (Adams, 1999; Collyer et al., 2020; Profico, Buzi, et al., 2019). The solution provided in Arothron, *combinland*, consists of appending the PC scores coming from different principal component analyses (PCAs) performed on each region (or view) to be combined after applying a normalization (the landmark coordinates are divided by the square root of the number of landmarks times the number of dimensions). In combining two landmark configurations (F and S), *combinland* divides their respective centroid sizes (CS_F and CS_S) by \sqrt{km} (as proposed in Dryden & Mardia, 2016, section 2.2.2), where k and m are respectively the number of landmarks and the number of dimensions (2D or 3D).

$$CS^F = \frac{CS_F}{\sqrt{k_F m_F}}$$

$$CS^S = \frac{CS_S}{\sqrt{k_S m_S}}$$

The normalization allows to combine landmark configurations avoiding distortions due to the unequal number of variables used in the different regions (or views). Recently, coordinate normalization has been criticized by Collyer et al. (2020). In this paper, we analyzed two different data sets either applying or omitting the normalization factor. The case study consists of the combination of five anatomical 2D views defined on a primate cranial sample. We evaluated the performance of *combinland* by calculating the correlation between the PC



FIGURE 1 Three 3D models available in Arothron to extract virtual cavities. From left to right: A deciduous Neanderthal tooth (violet), a modern human malleus bone (orange), and a modern human cranium (light blue)

FIGURE 2 The case study under controlled condition embedded in the Arothron R package. A complete human cranium (orange) is converted into two disarticulated models (white)

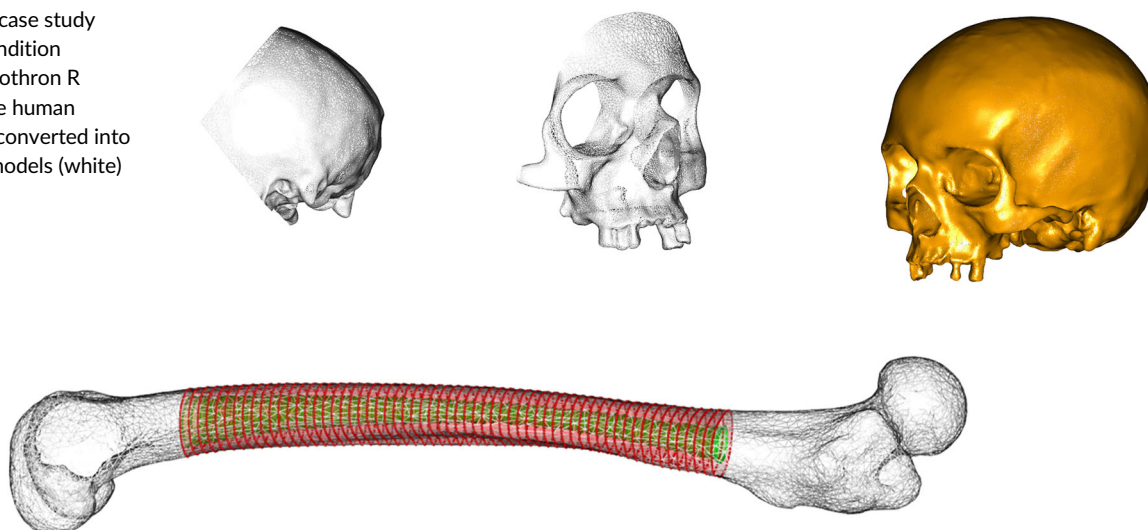


FIGURE 3 The femur case study used in evaluating the performance of *combinland*. The original data set, reported in the picture, composed by 61 cross-sections along 21 femoral diaphysis (100 equiangular semilandmarks on the periosteum and endosteum) is compared with three different data sets in which the number of endosteal semilandmarks varies (50 equiangular semilandmarks, 20 equiangular semilandmarks and 10 not equiangular semilandmarks)

scores obtained from the original 3D data set and the combined 2D data set. A second data set consists of semilandmarks acquired along the femoral periosteal and endosteal contours (Figure 3).

2.3 | Compare and visualize local differences in shape and size

Geometric Morphometrics comprises tools to visualize differences in shape and size between landmark configurations or surface meshes. Most of the available solutions to show differences in shape and size require a registration step (e.g., Procrustes registration). Commonly, shape differences are visualized by using a TPS algorithm (Bookstein, 1989) or by computing the (Euclidean) distance between landmarks and surface meshes. The main issue related to this approach is that the shape differences are expressed as a displacement leading to a misinterpretation of the real shape differences (Márquez et al., 2012; Piras et al., 2020). In Arothron, we propose a new solution to compute and visualize local differences between two surface meshes defined by the same topology (same triangulation of vertices). The function *localmeshdiff* calculates the area of each facet of the two surfaces, and returns the percentage change in the area of the reference mesh compared with the target mesh. The vector of surface area differences for the N facets is converted into a color vector of length N and charted on the reference mesh. The right and left tails of the distribution of surface area differences indicate local expansion and contraction, respectively. We tested the performance of *localmeshdiff* comparing the shape variations in modern humans between sexes by processing the same sample and defining on three examples 582, 1445, and 2927 semilandmarks, respectively.

We applied *localmeshdiff* to visualize differences in shape between the right brain hemisphere (i.e., endocast) of Neanderthals and modern humans (see Supplementary Code—*localmeshdiff*) (Profico, 2020).

3 | RESULTS

3.1 | Tools for extraction of virtual cavities: CA-LSE, AST-3D, and endomaker

The application of CA-LSE on a human malleus bone is presented to show how to obtain a 3D mesh of the complex network of blood vessels located within the external surface of this ear ossicle. The removal of the external surface of the ossicle reveals a bifurcating branch connected to the superior branch of the anterior tympanic artery through the nutrient foramen (Hamberger et al., 1963). This application shows the feasibility of a mesh-based approach to isolate and digitally reproduce complex skeletal cavities.

We applied AST-3D on a human skull. We defined a set of 30 points of view placed inside the endocranial cavity. AST-3D at each point of view starts a “scanning” process finding only those vertices visible from the point of view. The 3D virtual rendering of the resulting endocast is shown in Figure 4. The brain endocast built by Arothron reveals the shape of the endocast up to the fine details of the meningeal system and cranial nerves.

In the example, the application of Arothron provides a complete cranial endocast of the human skull in 10.57 s. The volume of the endocast is equal to 1355 cc.

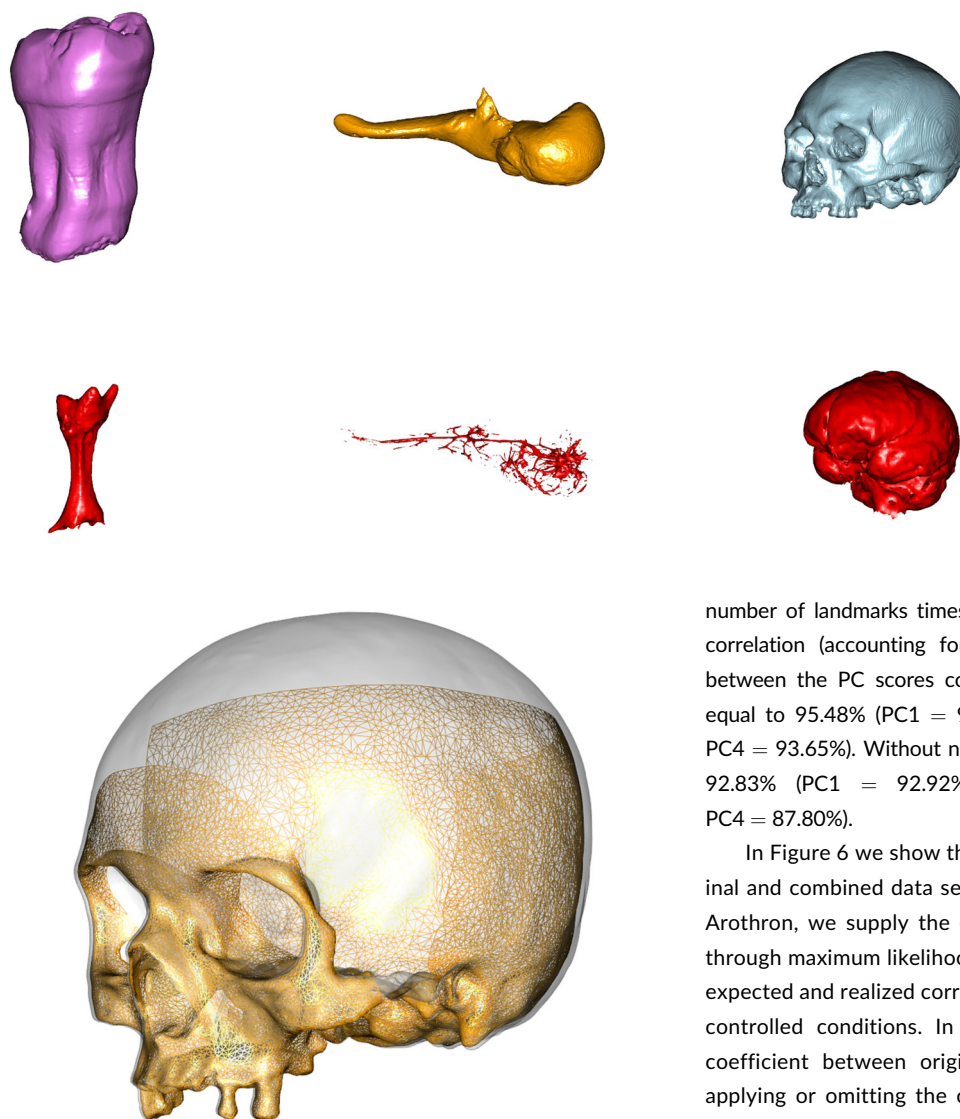


FIGURE 4 Outputs of the CA-LSE, AST-3d and *endomaker* tools applied on a deciduous Neanderthal tooth (violet), a modern human malleus bone (orange), and a modern human cranium (light blue). The extracted virtual cavities are shown in red

FIGURE 5 In orange the disarticulated model aligned after applying the DTA tool. In white the original model

3.2 | Combining morphological information from a 3D disarticulated model or from landmark configurations

We applied the DTA on a case study under controlled conditions: a complete human cranium has been converted into a disarticulated cranium in which the facial complex is separated from part of the neurocranium and cranial base. In this example, DTA found the individual named OL 1197 to be set as the reference sample (Figure 5). The average morphological distance between the two specimens is as small as 2.69 mm.

In the 2D primate case study we combined the morphological information of 28 primate species skulls acquired along five different anatomical views: anterior, posterior, superior, inferior, and right lateral. By applying the coordinate normalization proposed in Arothron (i.e., the landmark coordinates are divided by the square root of the

number of landmarks times the number of dimensions) we found a correlation (accounting for 75% of the total explained variance) between the PC scores coming from 3D and combined 2D views equal to 95.48% (PC1 = 95.33%, PC2 = 94.34%, PC3 = 98.59%, PC4 = 93.65%). Without normalization the total correlation drops to 92.83% (PC1 = 92.92%, PC2 = 92.20%, PC3 = 98.42%, PC4 = 87.80%).

In Figure 6 we show the correlation in shape between the original and combined data sets. In the currently accessible version of Arothron, we supply the estimation of the size correction factor through maximum likelihood by minimizing the difference between expected and realized correlation coefficients in experiments under controlled conditions. In addition, we calculate the correlation coefficient between original and combined data set by either applying or omitting the correction proposed in Arothron. In the femora case study, when the complete periosteum (100 equiangular semilandmarks) is combined with the endosteum (50, 20, and 10 equiangular semilandmarks) by applying the size correction the correlation with the original data set is equal to 1 in all three data sets. Omitting the correction of the coordinates by the number of variables correlation drops to 0.930, 0.718, 0.663, respectively.

The function *localmeshdiff* is specifically designed to visualize local variations in area from a reference surface to a target surface. Figure 7 describes the mean group differences between males and females by comparing three pairs of surface meshes containing a different number of vertices (582, 1445, and 2927). In all the three examples the zygomatic process, the mastoid, and the region defined by the frontal trait of the temporal line (i.e., between the frontozygomatic and the stephanion) are more expanded in males (Figure 7). In the example reported in Figure 8 we ran *localmeshdiff* to plot the differences between the Neanderthal and modern human brain morphology. The modern human right hemisphere, compared to the Neanderthal morphology, appears more expanded in the temporoparietal region. On the contrary the frontal lobe is more stretched in Neanderthals except for a small region

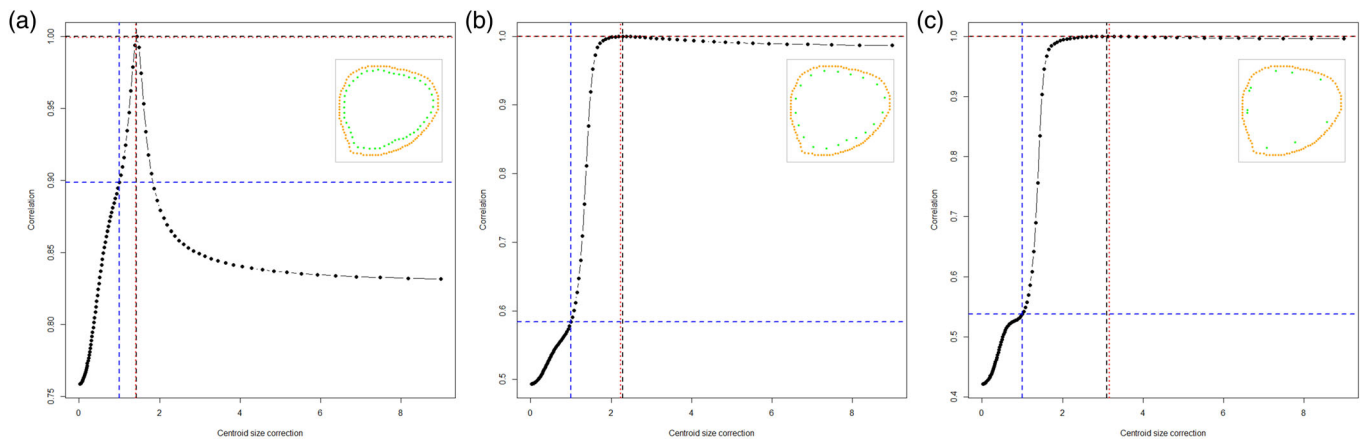


FIGURE 6 Performance of *combinland* in combining the morphological information by using a case study under controlled conditions. In 21 human femora the periosteum (100 semilandmark) is combined respectively with 50 equiangular semilandmarks (a), 20 equiangular semilandmarks (b), and 10 random semilandmarks (c). On the x-axis of each graph is reported the size correction tested and on the y-axis the correlation with the original data set. The red and blue dashed lines represent respectively the performance of *combinland* applying or omitting the size correction available in the Arothron R package

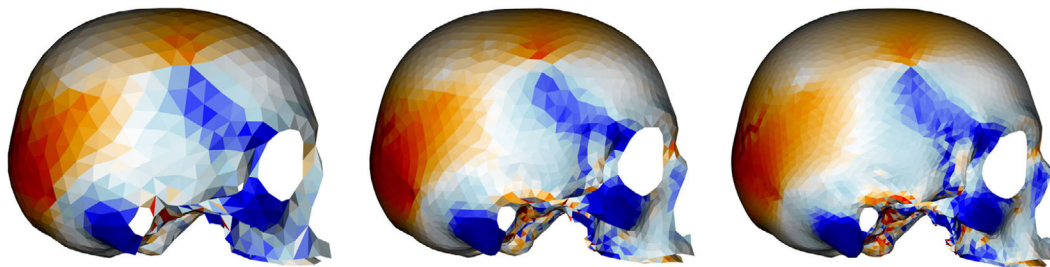
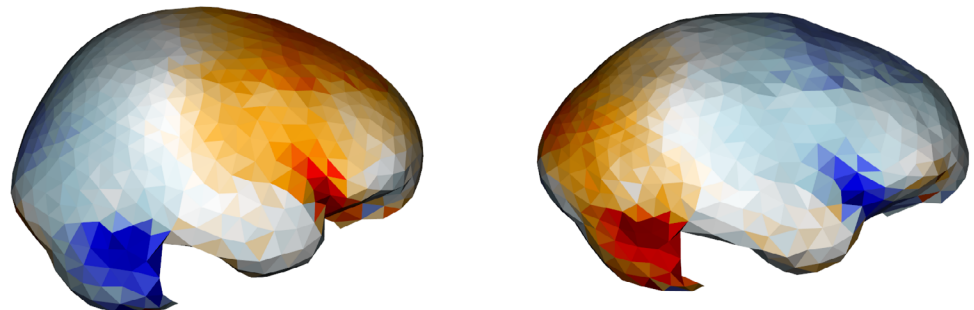


FIGURE 7 Local variation between male and female crania defining different number of surface semilandmarks. From the left to the right the surface meshes are built by using 582, 1445 and 2927 semilandmarks. Cold colors indicate expansion of area, warm colors show local contraction

FIGURE 8 The function *localmeshdiff* has been applied to map the morphological differences in shape of the right hemisphere between *Homo sapiens* and *Homo neanderthalensis* (on the left) and vice versa (on the right). Cold colors indicate expansion of area, warm colors show local contraction



characterized by a local contraction in the anterolateral part of the frontal lobe.

4 | DISCUSSION

The analysis of shape variation at different levels, from single individuals to the largest (macroevolution) scale is the domain of evolutionary studies. Unfortunately, this enterprise is limited by the scant information coming from the fossil record, which is otherwise crucial as even partially erroneous fossil information allows better

understanding of evolutionary patterns than ignoring fossil specimens altogether (Puttick, 2016; Webster & Purvis, 2002). The fossil record only represents a little fraction of past phenotypic diversity, and even this low percentage comes incomplete, deformed, and literally broken into pieces. On top of this, by virtue of their importance, rarity, and fragility, human fossil remains are not easily accessible, so that the most scientists are not allowed to study them directly. During the last decades, the increasing availability of 3D models obtained by means of computed tomography (CT), laser scanning, or photogrammetry has expanded the availability of fossil specimens. Yet, their quality and the possibility to look at the

original phenotypes remain limited. The R package Arothron was meant to restore and inspect in fine detail such past diversity. Performing the virtual restoration and rendering of fossil specimens that have suffered the impact of taphonomic processes befallen on them is currently possible, but the procedures are slow and prone to biases due to the user level of expertise and the subjective interpretation of morphological variation. In Arothron, we supply functions able to articulate damaged specimens, to combine the morphological information recorded on different part of the same organisms, to extract the inner structures of the specimens in a mathematically driven, fully automatic way. The visualization of shape difference among three-dimensional structures is challenging in morphological comparisons because traditional approach considers the relative positions of 3D models' facets subjected to variation due to the different registration method used. The solution we embedded in Arothron is completely free by coordinates registration taking into account only local variation between the reference and the target surface.

ACKNOWLEDGMENTS

The authors thank the curator and institutions that permitted access to the osteological collections. We are grateful to Prof. J. Moggi Cecchi and Dr. M. Zavattaro (Museum of Anthropology of Florence), Prof. G. Manzi (Museum of Anthropology of Rome "G. Sergi"). We thank Prof. Paul O'Higgins for his advice during the development of the function *localmeshdiff*. We thank Antonietta Del Bove for supplying the example data on modern human cranial morphology. The authors want to express their gratitude to the four anonymous reviewers who helped improving the manuscript with their useful comments.

CONFLICT OF INTEREST

The authors declare that there is no conflict of interest.








AUTHOR CONTRIBUTIONS

Antonio Profico: Conceptualization-Lead, Data curation-Lead, Formal analysis-Lead, Investigation-Lead, Methodology-Lead, Project administration-Lead, Software-Lead, Validation-Lead, Visualization-Lead, Writing-original draft-Lead, Writing-review & editing-Lead. **Buzi Costantino:** Data curation; methodology; software; writing-review & editing. **Castiglione Silvia:** Data curation; validation; visualization; writing-review & editing. **Melchionna Marina:** Formal analysis; methodology; software; validation; visualization; writing-original draft; writing-review & editing. **Piras Paolo:** Formal analysis; investigation; methodology; software; writing-review & editing. **Veneziano Alessio:** Data curation; methodology; software; writing-review & editing. **Raia Pasquale:** Conceptualization; formal analysis; investigation; methodology; project administration; software; supervision; writing-original draft; writing-review & editing.

DATA AVAILABILITY STATEMENT

Supplementary code and full data are available on Zenodo (<https://doi.org/10.5281/zenodo.4114233>).

ORCID

Profico Antonio  <https://orcid.org/0000-0003-2884-7118>
Buzi Costantino  <https://orcid.org/0000-0001-8951-2990>
Castiglione Silvia  <https://orcid.org/0000-0002-6140-1495>
Melchionna Marina  <https://orcid.org/0000-0001-7919-4431>
Piras Paolo  <https://orcid.org/0000-0001-9832-2742>
Veneziano Alessio  <https://orcid.org/0000-0002-2543-5188>
Raia Pasquale  <https://orcid.org/0000-0002-4593-8006>

REFERENCES

- Adams, D. C. (1999). Methods for shape analysis of landmark data from articulated structures. *Evolutionary Ecology Research*, 1(8), 959–970.
- Bookstein, F. L. (1989). Principal warps: Thin-plate splines and the decomposition of deformations. *IEEE Transactions on Pattern Analysis and Machine Intelligence*, 6, 567–585.
- Castiglione, S., Serio, C., Mondanaro, A., Melchionna, M., Carotenuto, F., di Febraro, M., Profico, A., Tamagnini, D., & Raia, P. (2020). Ancestral state estimation with phylogenetic ridge regression. *Evolutionary Biology*, 47(3), 220–232.
- Collyer, M. L., Davis, M. A., & Adams, D. C. (2020). Making heads or tails of combined landmark configurations in geometric morphometric data. *Evolutionary Biology*, 47, 193–205.
- Cunningham, J. A., Rahman, I. A., Lautenschlager, S., Rayfield, E. J., & Donoghue, P. C. J. (2014). A virtual world of paleontology. *Trends in Ecology & Evolution*, 29(6), 347–357. <https://doi.org/10.1016/j.tree.2014.04.004>
- Dryden, I. L., & Mardia, K. V. (2016). *Statistical shape analysis, with applications in R* (Second ed.). John Wiley and Sons Ltd.
- Gunz, P., Mitteroecker, P., Neubauer, S., Weber, G. W., & Bookstein, F. L. (2009). Principles for the virtual reconstruction of hominin crania. *Journal of Human Evolution*, 57(1), 48–62.
- Hamberger, C. A., Marcuson, G., & Wersäll, J. (1963). Blood vessels of the ossicular chain. *Acta Oto-Laryngologica*, 56(sup183), 66–70.
- Joy, J. B., Liang, R. H., McCloskey, R. M., Nguyen, T., & Poon, A. F. Y. (2016). Ancestral reconstruction. *PLoS Computational Biology*, 12(7), e1004763.
- Katz, S., Tal, A., & Basri, R. (2007). Direct visibility of point sets. *ACM Transactions on Graphics (TOG)*, 26, 24.
- Márquez, E. J., Cabeen, R., Woods, R. P., & Houle, D. (2012). The measurement of local variation in shape. *Evolutionary Biology*, 39(3), 419–439.
- Pandolfi, L., Raia, P., Fortuny, J., & Rook, L. (2020). Evolving virtual and computational paleontology. *Frontiers in Earth Science*, 8, 479.
- Piras, P., Profico, A., Pandolfi, L., Raia, P., di Vincenzo, F., Mondanaro, A., Castiglione, S., & Varano, V. (2020). Current options for visualization of local deformation in modern shape analysis applied to paleobiological case studies. *Frontiers in Earth Science*, 8, 66.
- Profico, A. (2020). Code and data to reproduce case studies embedded in the Arothron R package. Zenodo. <https://doi.org/10.5281/zenodo.4114233>
- Profico, A., Buzi, C., Davis, C., Melchionna, M., Veneziano, A., Raia, P., & Manzi, G. (2019). A new tool for digital alignment in virtual anthropology. *The Anatomical Record*, 302(7), 1104–1115.
- Profico, A., Buzi, C., Melchionna, M., Veneziano, A., & Raia, P. (2020). Endomaker, a new algorithm for fully automatic extraction of cranial endocasts and the calculation of their volumes. *American Journal of Physical Anthropology*, 172, 511–515.
- Profico, A., Piras, P., Buzi, C., Del Bove, A., Melchionna, M., Sansalone, G., Varano, V., Veneziano, A., Raia, P., & Manzi, G. (2019). Seeing the wood through the trees. Combining shape information from different landmark configurations. *Hystrix, the Italian Journal of Mammalogy*, 30(2), 157–165.

- Profico, A., Schlager, S., Valoriani, V., Buzi, C., Melchionna, M., Veneziano, A., Raia, P., Moggi-Cecchi, J., & Manzi, G. (2018). Reproducing the internal and external anatomy of fossil bones: Two new automatic digital tools. *American Journal of Physical Anthropology*, 166, 979–986. <https://doi.org/10.1002/ajpa.23493>
- Puttick, M. N. (2016). Partially incorrect fossil data augment analyses of discrete trait evolution in living species. *Biology Letters*, 12(8), 20160392.
- Schnitzler, J., Theis, C., Polly, P. D., & Eronen, J. T. (2017). Fossils matter—understanding modes and rates of trait evolution in Musteloidea (Carnivora). *Evolutionary Ecology Research*, 18(2), 187–200.
- Slater, G. J., Harmon, L. J., & Alfaro, M. E. (2012). Integrating fossils with molecular phylogenies improves inference of trait evolution. *Evolution: International Journal of Organic Evolution*, 66(12), 3931–3944.
- Weber, G. W. (2001). Virtual anthropology (VA): A call for Glasnost in paleoanthropology. *The Anatomical Record*, 265(4), 193–201. <https://doi.org/10.1002/ar.1153>
- Webster, A. J., & Purvis, A. (2002). Testing the accuracy of methods for reconstructing ancestral states of continuous characters. *Proceedings of the Royal Society of London. Series B: Biological Sciences*, 269(1487), 143–149.
- Wood, B., & Richmond, B. G. (2000). Human evolution: Taxonomy and paleobiology. *Journal of Anatomy*, 197(1), 19–60.

How to cite this article: Antonio, P., Costantino, B., Silvia, C., Marina, M., Paolo, P., Alessio, V., & Pasquale, R. (2021). Arothron: An R package for geometric morphometric methods and virtual anthropology applications. *American Journal of Physical Anthropology*, 176(1), 144–151. <https://doi.org/10.1002/ajpa.24340>